Short-range order of titania doped silica sono-aerogel

Luis Esquivias *, Milagrosa Ramirez Del Solar

Departamento de Física de la Materia Condensada, Facultad de Ciencias, Universidad de Cádiz, Apartado 40, Puerto Real, 11510 Cadiz, Spain

Abstract

The atomic arrangements around Ti atoms in titania doped silica gels were studied by X-ray absorption spectroscopy. The gels were prepared by ultrasonic treatment of an alkoxide and acidic water mixture (sonogel) and conventionally in alcoholic solution. From the comparison of gels, XANES spectra with those of $SrTiO_3$, anatase and rutile TiO_2, an octahedral environment of Ti in the SiO_2 network can be inferred. These octahedra are distorted as in the case of TiO_2. Ti did not occupy the Si sites but rather accumulated in domains where the Ti atoms are especially abundant. The sonogel network is formed up to the second neighbor level, contrary to the classic gel in which no coordination spheres can be made out above the first neighbor sphere. © 1997 Elsevier Science B.V.

1. Introduction

One of the outstanding features commonly attributed to the sol–gel processing of multicomponent materials is the high degree of homogeneity at a molecular scale. Thus, from the pioneering times of sol–gel research, a considerable amount of effort was headed toward the preparation of mixed glasses, impossible to obtain by standard methods. One of the most studied systems was TiO_2–SiO_2, especially because glasses of this system have a low thermal expansion coefficient and gels can be used as catalyst support for strong metal–support interaction [1] devices. After several years of inactivity of the basic research in this field, interest in TiO_2–SiO_2 is recovering. This is probably due to rediscovered possibili-

ties such as, for example, thin films for use as planar waveguides [2]. Much work occurred between the last two Workshops on Glasses and Ceramics from Gels to characterize the structure and kinetics of these mixed gels [3–5].

Kamiya et al. [6] reported that homogeneity can be obtained in a substitutional solution of TiO_2 in SiO_2 in the range 0–8.9 mol%. In this stable region, from room temperature to 1000°C, Ti is fourfold coordinated. For increasing Ti concentration, octahedral Ti coordination, is observed. Everybody agrees that titanium predominantly assumes a tetrahedral coordination in the high silica region and in the low silica region octahedral coordination prevails. It seems that, for a fixed TiO_2, Ti coordination depends on the preparation method. Emili et al. [7] attributed the discrepancies of their results with those of Sandstrom et al. [8], prepared by flame hydrolysis, to more homogeneous prepared materials. They assume that if TiO_2 is completely dissolved in the

* Corresponding author. Tel.: +34-56 830 966/210; fax: +34-56 837 205/4924; e-mail: luis.esquivias@uca.es.

SiO_2 network, Ti is occupying Si sites and, therefore, the nearer the average Ti coordination is to 4, the more homogeneous the solid solution is. Thus, it seems that a short-range order around a Ti atom can give information on homogeneity. This could be a simplistic view but it does not have to be far from the actual situation, especially in the low silica region.

Extended X-ray absorption fine structure (EXAFS) is a powerful probe that allows structural characterization around a localized atomic specie, even in the case where it is very dilute. Because of its selectivity, if the short-range orders of the involved species are different enough, it can be use to study the homogeneity of the material at an atomic level. It can be done from the Fourier transform of the EXAFS function that gives a pseudo radial distribution function (PRDF) around an arbitrary atom. It would be great to have EXAFS experimental data on the oxygen K edge because it is around this atom that homogeneity can be perceived. However, only near-edge data can be obtained since it is not possible to have an absorption spectrum extended enough to have a number of oscillations permitting the calculate of a PRDF.

We have used the spectra and structure of TiO_2 crystals such as rutile and anatase and a perovskite type ($SrTiO_3$) for comparison. In rutile and anatase, titanium is surrounded by octahedral oxygen. The difference lies in the number of shared edges by two adjacent octahedra. There are two in rutile, leading to the characteristic corner-sharing octahedral chains (Ti_3O bridges) of the rutile structure and four in anatase, resulting in the typical skewed chains of the anatase structure. There are also six O atoms around Ti in the perovskite but, unlike the TiO_2 crystals, there is only one Ti–O distance because the oxygen octahedron is regular.

When the precursors of gels are alkoxides they are hydrolyzed and the solid phase results from the subsequent polycondensation process. In this case, homogeneity can only be satisfactorily reached if their respective hydrolysis and polycondensation reactions occur in a synchronized manner allowing the formation of mixed M–O–M′ bonds. We have reported that in the case of sonogels the cavitation phenomenon, which is responsible for the alkoxide–water mixture homogenisation, accelerates hydroly-

sis [9]. The solventless processing deeply affects the condensation rate and, consequently, as it has been verified, affects both short-range-order and textural characteristics [10]. Between them, the more particular since sonogels are formed by a uniformly sized distribution of elementary particles of approximately 1 nm radius [11]. The purpose of this work is to delve into the influence of the sonocatalysis on the atomic short-range order.

2. Experimental

Silica gels doped with a 5 mol% titania were prepared by mixing solutions of oxide precursors, tetraethoxysilane (TEOS) and tetrabutylorthotitanate (TBOT). The chemical reactions were carried out under acidic conditions with a pH [HCl] = 1.5.

In the sonocatalytic method, the solventless TEOS–water mixture was submitted to ultrasonic radiation produced by a sonifier (Vibracell, Sonics and Materials, USA), operating at 20 KHz with a titanium transducer of 13 mm diameter driven by an electrostrictive device [12]. Once the resulting sonosol was cooled to 0°C, a solution containing titanium precursor $Ti(OBu^n)_4$ (TBOT) was added drop by drop to obtain the desired composition. In this solution [TBOT]:[BuOH]:[AcOH] 1:3.5:1.5, the reactivity of titanium alkoxide was decreased by chelation with acetic acid [13]. As comparison, classic silica sols with the same composition were also prepared, under magnetic stirring, in alcoholic (EtOH) dilution and doped with the same amount of TiO_2.

Homogeneous liquids were poured in glass hermetic containers at 50°C and held until gelation. Hypercritical drying of the wet gels in an autoclave ($p = 190$ bar and $T = 300$°C) leads to monolithic aerogels [14]. Oxidation of the remaining organic groups for 5 h and dehydration by means of chlorinating for 8 h were accomplished at 500°C. Thermogravimetry indicated that these treatments removed unwanted residues.

'S' refers to a sample prepared using ultrasound to mix the two phases of the alkoxide–water system. When ultrasounds are not employed and ethanol was used as solvent to obtain a homogeneous solution, the sample will be referred to as 'C'.
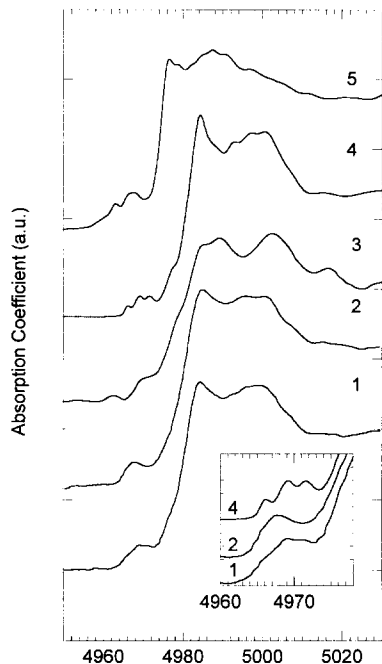
Fig. 1. Ti K-edge room temperature XANES spectra of: (1) silica sono-aerogel doped with titania at 5 mol%, (2) silica aerogel doped with titania at 5 mol%, prepared in alcoholic solution, (3) rutile, (4) anatase and (5) $SrTiO_3$.

XAS measurements were made at room temperature on a beam line XAS3 at the D.C.I. storage ring (Orsay, France) using the quick-scanning EXAFS (QEXAFS) acquisition operative mode [15] adapted for this station by Prieto et al. [16]. The integration time has been proven to be small enough in a way that it is smaller than the time of flight corresponding to each points of the spectrum. Data were collected with a fixed exit monochromator using two flat Si(311) crystals in transmission mode. Detection was made by using two ion chambers with air as fill gas and a photomultiplier with a scintillation plastic for the fluorescence yield detection. Energy resolution was estimated to be about 0.3 eV by the Cu foil 3d near edge feature. The energy calibration was monitored using the Ti foil sample and was set as 4965 eV at the first maximum of the derivative spectrum. EXAFS spectra were performed over a range of 800 eV above the Ti K-edge with 2 eV resolution. Raw data were smoothed with the subrou-

tine R_SMOOT [17]. EXAFS and XANES analysis procedures were already described [18].

To evaluate the neighbor's position around the absorber atoms, the well known theoretical EXAFS function, $\chi(k)$, in the single scattering theory and in the plane-wave approximation was used [19]:

$$\chi(k) = \sum_j \frac{N_j}{R_j^2} \exp\left(-2k^2\sigma_j^2\right) \exp\left(\frac{\Gamma_j R_j}{k}\right) f_j$$

$$\sin\left[2kR_j + \varphi_j(k)\right]. \tag{1}$$

$k = [2m_e/\hbar^2(E - E_0)]^{1/2}$ is the photoelectron wave vector modulus, m_e being the electron mass and E_0 the threshold energy. As usual, an approximate energy value near the edge (E_{0_i}) was initially assigned to $k = 0$. Then, during fitting, $\Delta E_0 = E_0 - E_{0_i}$ is treated as an additional parameter. N_j is the average coordination number for the Gaussian distribution of distances centered at R_j. σ_j is the Debye–Waller contribution, $\varphi_j = 2\delta(k) + \gamma_j(k)$ is the phase shift, $\delta(k)$ and $\gamma_j(k)$ being, respectively, those of the central and backscattering atoms. f_j is the amplitude
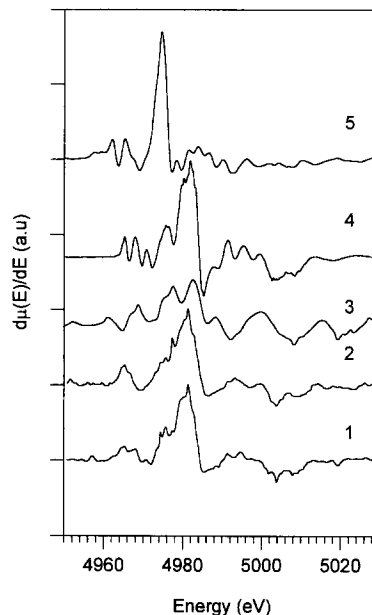

Fig. 2. First derivative of Ti K edge XANES spectra. (1) silica sono-aerogel doped with titania at 5 mol%, (2) silica aerogel doped with titania at 5 mol%, prepared in alcoholic solution, (3) rutile, (4) anatase and (5) $SrTiO_3$.
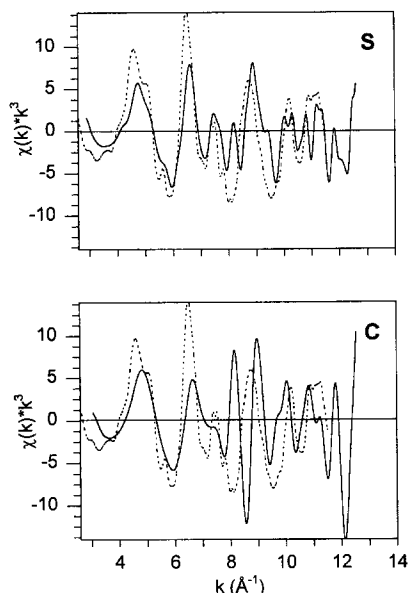
Fig. 3. Room temperature EXAFS spectra of Ti K-edge for silica classic aerogel (top) and sono-aerogel (bottom) doped with titania at 5 mol%. The dotted lines represent that of the anatase.

Fig. 4. Fourier transform of Ti k^3EXAFS weighted signals for silica aerogels doped with titania at 5 mol%. Sonogel (continuous thin line), classic gel (dashed line) and anatase (continuous bold line).

of the backscattering atoms, $\Gamma_j = k / \Lambda(k)$, $\Lambda(k)$ being the photoelectron mean free path. To estimate the shift caused by the scattering phase [20] $f_j(k)$ and $\varphi_j(k)$ have been theoretically calculated by the method reported by Rehr et al. [21] which include a calculation of $\Lambda(k)$. To avoid spurious oscillations FT were calculated with a Hanning window selecting the transform range from 3 to 13 Å. The Fourier transform (FT) of $k^3\chi(k)$ is the pseudo radial distribution function (PRDF), called so because the actual nearest neighbour distances are shifted slightly toward longer distances and thus the radial positions are only approximate or pseudodistances [22]. Data
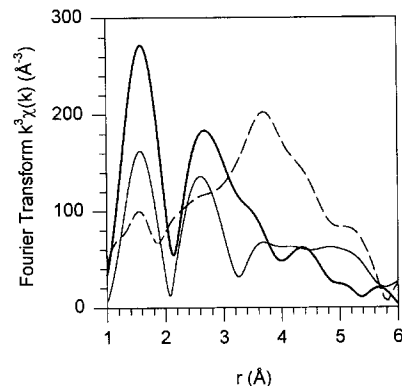
have been fitted in the k- and R-spaces by comparison of experimental data filtered (to extract the EXAFS contribution of the coordination sphere) and spectra calculated by Eq. (1).

For all the XANES spectra a Victoreen law, extrapolated from the low energy region, has been subtracted and then the normalisation performed.

3. Results

In Fig. 1 the XANES spectra of the studied samples are represented beside the standard used as references. The absorption coefficient derivatives are represented in Fig. 2. The sample spectra show features at 4985 and 5000 eV like anatase, however they do not present the characteristic triplet at the pre-edge but a wide hump. The edge width of the C

Table 1
EXAFS result of silica gels doped with titania at 5 mol%

Sample	Bonding	ΔR (Å)	Δk (Å^{-1})	N_{CN}	R (Å)	σ^2 (Å^2)	ΔE_0 (eV)	ε * (%)
S	Ti–O	1.2–2.0	3.1–12.4	2	1.91	0.0030	−27.02	3.5
	Ti–Ti	2.1–3.2	31–11.2	6	2.95	0.0071	9.00	18.4
	Ti–Si			6	2.90			
C	Ti–O	1.3–1.9	3.3–12.4	1	1.87	0.0009	−27.02	6.2
Anatase	Ti–O	1.1–2.1	2.8–11.4	6	1.97	0.0081	−25.08	12.8

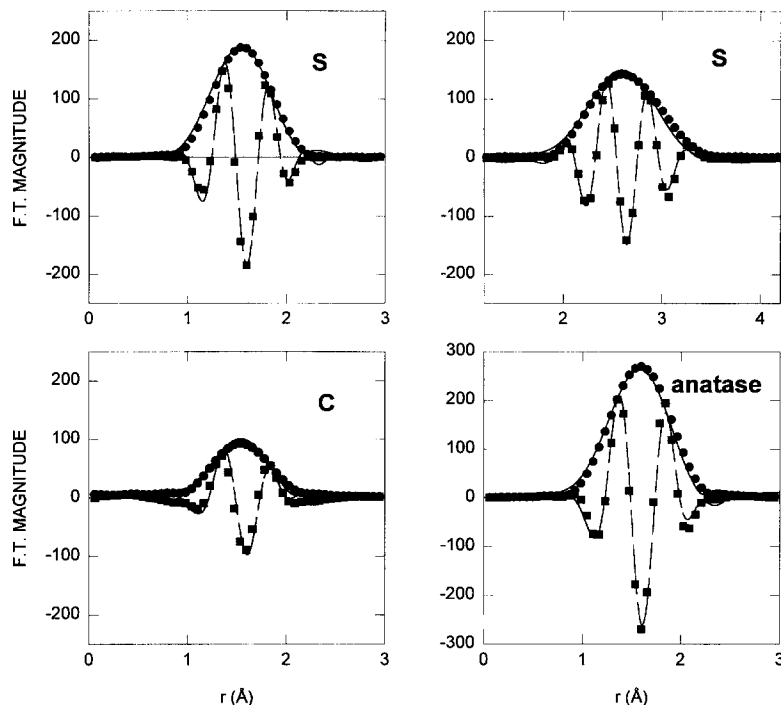$\varepsilon = \Sigma(k^3\chi(k)_{exp} - k^3\chi(k)_{calc})^2 / \Sigma(k^3\chi(k)_{exp})^2$.

Fig. 5. Comparison of experimental (points) with calculated (continuous line) modulus and imaginary part of the filtered data in R-space at Ti K-edge for Ti–O shell of the sonogel (left top), classic gel (left bottom) and anatase (right bottom) samples and Ti-cation of the sonogel sample (right top).

sample spectrum is narrower than that of the S sample but both are wider than the anatase one. The oscillation amplitudes are lower than in the spectrum of anatase.

A different local order around Ti atoms is inferred from the shape and amplitude of the EXAFS spectra Ti K-edge, shown in Fig. 3. This situation is coherent with the PRDF profile (Fig. 4). S shows two defined peaks, corresponding to Ti–O and Ti-cation distances. C's PRDF shows a weak first peak and several overlapped second neighbor peaks.

Fourier transform filtering was used to extract the EXAFS contribution of the first coordination sphere which is an assumed monolayer (only O atoms around Ti) resulting in the isolation of the Ti–O shell in $k^3\chi(k)$. Fig. 5 shows the fits obtained in the real space. The second peak of S's PRDF was considered defined enough to try a fitting. It could be fitted under a two shell hypotheses of Ti and Si. Neither Ti–Ti nor Ti–Si one shell fitting was satisfactory. Table 1 abridges the results of the fittings. The uncertainty of coordination numbers has been esti-

mated to be roughly 20% [23]. A uncertainty of approximately ± 0.02 Å is generally assigned to the neighbor distances measured by EXAFS [24].

4. Discussion

The S and C samples' XANES signals are assimilated to the anatase one at a great extent. The position and height of the features 4985 and 5000 eV for both samples are very similar to anatase notably in S sample (Fig. 1). This means that most of their Ti ions are Ti (IV). In octahedral symmetry, Ti is characterized by a weak triplet in the pre-edge region. The origin of the first one of this series is not well known but the two peaks located at a higher energy correspond to $1s \rightarrow 3d$ transitions which are forbidden in a structure with a centre of symmetry. The presence of a centre of inversion, as in a tetrahedral symmetry, gives rise to a unique and intense peak [25,26]. The hump in the S sample clearly corresponds to an overlapping of the peaks that forms the triplet caused by the short-range disorder.

It permits practically the ruling out of the presence of tetrahedral sites in this sample. The same cannot be said for the C sample as can be seen in the inset in Fig. 1. In this case the hump is sharper and situated at a lower energy than the maximum of its sono-counterpart and, consequently, the presence of tetrahedral sites has not been discarded. The absorption coefficient derivatives are more eloquent regarding some aspect of the local order (Fig. 2), especially those concerning edge width. The edge width as well as the oscillation amplitude is a feature commonly associated with the coordination of the probe-backscatterer atoms. The wider the edge and the lower the oscillation amplitudes the higher the covalent character of this bond, and, therefore, the lower the coordination. This conclusion does not seem relevant since the covalent characters of the Ti–O bond in the gels and in anatase are the same. However, the edge width is also related to the absorber symmetry as it defines the splitting of the degenerate energy levels. Therefore, the edge width should be small for highly symmetric coordination as is the case of $SrTiO_3$. Thus, the O arrangement around the Ti ions basically consist of distorted octahedra, especially in the C sample, although there could coexist with some Ti tetrahedrally coordinated.

The Ti K edge PRDF of the S sample presents a first peak higher than that of C, indicating a higher short-range order around the Ti atoms. A striking characteristic of the S's PRDF (Fig. 4) is the existence of a defined peak corresponding to the cation–cation distance which is not in C. Its short-range order up to the next nearest neighbours scale is quite similar to the anatase one, just having the peaks a lower amplitude. The aspects of the $k^3 * EXAFS$ functions already suggest that the short-range order of the S sample looks more like the anatase than the C sample does. The low Ti–O shell amplitude of the C sample hints a very poor atomic order at this level.

For the fitting we have assumed, from Shannon's table of ionic radii [27], that the Ti–O bond length in the amorphous sample is 2.08 Å. Since interatomic distances are highly correlated to ΔE_0, the R_j value, once N_{CN} was fixed at a reasonable integer, was used to obtain the best fit to the experimental data of S and C samples. The same as in other Ti oxides, the Ti atoms coordination number was fixed to 6. Then, R_j and σ_j allowed the float up to obtain a good

fitting. The best fit to the Ti–O shell of the S sample gives a shorter bond length (1.91 Å) and an average coordination much lower than the starting value. This bond length is a little longer than some reported values for glasses of this system with approximately the same composition. However the coordination number is extremely low. This can be attributed to a structure of TiO_6 units in which the furthest O atoms cannot be seen at room temperature because it corresponds to loose Ti–O bonds. The same effect has been reported by Ping-Li et al. [28] for tetragonal yttria doped zirconia. Only the inner Zr–O subshells were observed at room temperature, contrary to what happens at 10 K. The outer subshell disappears because of the increased disorder in these longer, looser bonds. The C sample is fitted with a lower coordination number and bond length, indicating a disorder still higher. Accordingly, the Debye–Waller factor is very low ($\sigma^2 \sim 10^{-3}$ Å^{-2}) for this particular atom. We also fitted it with $N_{CN} = 4$, $\sigma^2 = 1.9 \cdot 10^{-2}$ Å^{-2} and $\varepsilon^2 = 12.5$ but their counterpart in R-space was not satisfactory. As in X-ray diffraction, σ is a vibrational disorder factor but with a different physical meaning. In XRD, it features the thermal motion of every individual atom, whereas in EXAFS, it represents the distribution of the absorber-backscatterer distance with respect to absorber atom. These results indicate that in such disordered networks, both descriptions are equivalent: few neighbours with a very low thermal disorder with respect to the central atom or a high number of first neighbours very disordered. The description we give in this paper means that only 1 (C) or 2 (S) neighbors have bonds fastened enough to be 'seen' by the central atom. The contribution of the rest is diluted as a background of the X-ray absorption spectrum. We made a single shell fitting the PRDF anatase first peak in which Ti is also coordinated by oxygens, having two non-equivalent Ti–O distances (Table 1 and Fig. 5). We found the standard values for coordination and the average nearest neighbour distance. This supports the reliability of the employed analysis method and corroborates the hypothesis of a very disordered arrangement of O around Ti. This disorder is not just because of their amorphous character but also increased as an effect of their high surface to volume ratio.

The S sample next nearest neighbors peak could

only be fitted with two shells of Ti and Si. The distribution of Si and Ti atoms (fifty–fifty) does not agree with that expected for a statistically random distribution in a homogeneous structure. The resulting next near neighbor distance represent an important deviation from the predictable values for this system.

5. Conclusions

(1) The Ti coordination is slightly affected by the preparation method. In all cases, the majority of them are hexacoordinated forming very distorted octahedra with loose bonds, looser in the classic gel although in this case the number of tetrahedral sites is not negligible.

(2) The short-range order at the scale of second neighbours is influenced by the preparation method. The sonogel route gives a less disordered network than the classic one presenting an atomic structure near to that of the bulk glass.

(3) The arrangement of the Ti atoms throughout the S sample silica structure does not correspond to a perfect statistical distribution but rather accumulated in domains where the Ti atoms are especially abundant.

Acknowledgements

References

[1] M.A. Cauqui, J.J. Calvino, G. Cifredo, L. Esquivias, J.A. Pérez, J.M. Rodríguez-Izquierdo, J. Non-Cryst. Solids. 147& 148 (1992) 758.

[2] X. Orignac, H.C. Vasconcelos, X.M. Du, R.M. Almeida, J. Sol–Gel Sci. Technol. 8 (1-3) (1997) 243.

[3] J. Livage, ed., J. Sol–Gel Sci. Technol. 2 (1–3) (1994).

[4] R.M. Almeida, ed., J. Sol–Gel Sci. Technol. 8 (1–3) (1997).

[5] G.S. Henderson, M.E. Fleet, J. Non-Cryst. Solids 211 (1997) 214.

[6] K. Kamiya, S. Sakka, N. Tashiro, Yoguio-Kyokai-Shi 84 (1976) 614.

[7] M. Emili, L. Incoccia, S. Mobilio, G. Fagherazzi, M. Guglielmi, J. Non-Cryst. Solids 74 (1985) 129.

[8] D.R. Sandstrom, F.R. Lytle, P.S. Wei, R.B. Greegor, J. Wong, P. Schultz, J. Non-Cryst. Solids 41 (1980) 201.

[9] M. Ramírez-del-Solar, L. Esquivias, A.F. Craievich, J. Zarzycki, J. Non-Cryst. Solids 147&148 (1992) 40.

[10] E. Blanco, M. Ramírez del Solar, L. Esquivias, A.F. Craievich, J. Non-Cryst. Solids 147&148 (1992) 296.

[11] J.M. Ruiz-Rube, M. Ramírez-del-Solar, N. de la Rosa-Fox, L. Esquivias, in: Basic Features of the Glassy State, Proc. 2nd Int. Workshop on Non-Crystalline Solids, ed. J. Colmenero and A. Alegría (World Scientific, Singapur, 1990) p. 69.

[12] M. Ramírez-del-Solar, N. de la Rosa-Fox, L. Esquivias, J. Zarzycki, J. Non-Cryst. Solids 121 (1990) 84.

[13] S. Doeuff, M. Henry, C. Sanchez, J. Livage, J. Non-Cryst. Solids 89 (1987) 206.

[14] M. Prassas, J. Phalippou, J. Zarzycki, J. Mater. Sci. 19 (1984) 1656.

[15] R. Frahm, Nucl. Instrum. Methods A270 (1988) 578.

[16] C. Prieto, P. Lagarde, H. Dexpert, V. Briois, F. Villain, M. Verdaguer, Meas. Sci. Technol. 3 (1992) 325.

[17] N. Zotov, in: Proc. 2nd National Conf. on X-Ray Diffraction Methods (Sofia University, Sofia, 1985) p. 132.

[18] C. Jiménez-Solís, L. Esquivias, C. Prieto, J. Alloys Compounds 228 (1995) 188.

[19] K. Teo, in: Inorganic Chemistry Concepts 9 (Springer, Berlin, 1986).

[20] A.G. Mckale, B.W. Veal, A.P. Paulikas, S.K. Chan, G.S. Knapp, J. Am. Chem. Soc. 110 (1986) 3763.

[21] J.J. Rehr, J. Mutree de León, S.I. Sabinsky, R.C. Albers, J. Am. Chem. Soc. 113 (1991) 5135.

[22] M.J. Fay, A. Proctor, D.P. Hoffmann, D.M. Hercules, Anal. Chem. 60 (21) (1988) 1225A.

[23] P. Eisenberger, B. Lengler, Phys. Rev. B22 (1980) 3551.

[24] B.A. Bunker, E.A. Stern, Phys. Rev. B27 (1983) 1017.

[25] R.B. Greegor, F.W. Lytle, D.R. Sandstrom, J. Wong, P. Schulz, J. Non-Cryst. Solids 55 (1983) 27.

[26] C.A. Yarker, P.A.V. Johnson, A.C. Wright, J. Wong, R.B. Greegor, F.W. Lytle, J.N. Sinclair, J. Non-Cryst. Solids 79 (1986) 117.

[27] R.D. Shannon, Acta Crystallogr. A32 (1976) 751.

[28] P. Li, I. Wei-Che, J.E. Penner-Hahn, Phys. Rev. B48 (14) (1993) 10074.